California Fish and Wildlife, Fire Special Issue; 14-45; 2020

ORIGINAL RESEARCH

Sonoma County Complex Fires of 2017: Remote sensing data and modeling to support ecosystem and community resiliency

KASS GREEN[1], MARK TUKMAN[2], DYLAN LOUDON[2], ALLISON SCHICHTEL[3], KAREN GAFFNEY[3], AND MATTHEW CLARK[4]

[1] *Kass Green & Associates, 1101 High Court, Berkeley, CA 94708, USA*

[2] *Tukman Geospatial, 1955 Cleveland Ave. Suite 201, Santa Rosa, CA 95401, USA*

[3] *Sonoma County Agricultural Preservation and Open Space District, 747 Mendocino Ave., Santa Rosa, CA 95401, USA*

[4] *Sonoma State University, 1801 East Cotati Ave., Rohnert Park, CA 94928, USA*

**Corresponding Author: karen.gaffney@sonoma-county.org*

In the western U.S., long-term fire suppression has led to a build-up of surface and ladder fuels, increasing the severity of fires. Coupled with increased home building in the wildland urban interface and global climate change, much of the western U.S. is facing unprecedented risk of catastrophic wildland fires. Given the almost 30 million acres of forestland in California, and the impacts to human community health and safety and natural systems that stem from uncontrolled fires, it is imperative that we understand the underlying processes and conditions in the landscape that determine fire impacts. In October of 2017, Sonoma County, California experienced three significant fires that resulted in loss of life and property, as well as impacts to natural systems. Sonoma County Ag + Open Space—with support from a team of technical consultants and in partnership with NASA and other experts—researched the impacts of the fires to woody vegetation within areas that burned during wind-driven and non-wind driven events. Using high-resolution aerial imagery, we mapped canopy condition of woody vegetation and used machine learning techniques to determine the importance of landscape measures of vegetation structure, land cover type, topography, climate and weather, and nearness to streams as predictors of woody canopy condition for areas that burned during the October 2017 fires. Across the landscapes, riparian and mesic vegetation types exhibited the least canopy damage, followed by upland hardwood forest types. Shrub and upland conifer types exhibited the most canopy damage. Measures of vegetation structure derived from lidar data are the most important predictors of post-fire woody canopy condition, in addition to slope-aspect, proximate vegetation community types, and distance to streams. In general, the higher the density of shrubs and fire-adapted vegetation types, the higher the density of ladder fuels, and the greater the distance from streams, the higher the canopy damage. This study emphasizes the value of high resolution airborne lidar for mapping vegetation type and structure and building locations at a scale large enough to inform local management decisions. The study also documents pre- and post-fire baseline conditions to support the long-term evaluation of vegetation impacts and provides remote sensing and analysis tools to better plan for, manage, and mitigate future extreme wildfire through the lens of climate and extreme event resiliency, community safety and ecosystem health.

Key words: biodiversity, climate resiliency, data collaborations, fire, forest health, fuel loading, land conservation, land management, remote sensing, Sonoma County, vegetation structure, vegetation type

---

California's wildlands are critically important in maintaining the state's biological diversity, as well as providing myriad other benefits related to human health and vitality. Forested watersheds provide clean and abundant drinking water for millions of people, sequester substantial amounts of carbon, provide revenue and jobs from the sale of wood products, create opportunities for recreation, and are important scenic attributes in California's tourism economy.

In California, 15 of the most destructive wildfires in the state's history occurred in the last 20 years (CAL FIRE 2019). The underlying causes of these wildfires stem from a variety of factors, including climate change, tree disease, drought, and land-use policies, as well as over 100 years of fire suppression (Keane et al. 2002; Miller 2012; Smith et al. 2016). These landscapes are home to a diversity of plant and animal species as well as millions of people who live in rural watersheds or in the wildland urban interface (WUI). Given the fact that forests cover about a third the California landscape (USDA Forest Service 2014) and forest conditions are influenced by vast temporal and spatial scales, high quality remote sensing data and analysis is critical for efficiently and effectively managing forests for both ecosystem and human community resiliency.

Sonoma County, California is a million-acre county situated at the northern boundary of the San Francisco Bay Area and the southern boundary of the rural North Coast counties of Mendocino, Humboldt, and Del Norte (Figure 1). A biologically rich area with a high degree of endemism, Sonoma County's wildlands are characterized by a relatively undeveloped coastline, a diversity of geologic features, three sizable rivers (Russian, Petaluma, and Gualala), numerous creeks and streams, and a variety of vegetation types including forests, woodlands, grasslands, salt and freshwater wetlands, and the Geysers geothermal area.

In 1990, Sonoma County voters created the Sonoma County Agricultural Preservation and Open Space District (Ag + Open Space) to permanently protect the diverse agricultural, natural resource, and scenic open space lands of Sonoma County for future generations. Along with its partners, the agency has permanently protected over 49,000 ha (121,000 acres) of land in Sonoma County, using the best available science and data to prioritize its actions.

Figure 1. Location of Sonoma County in California, USA.

Sonoma Veg Map: Foundational Data

Ag + Open Space relies on high quality data, ongoing analysis and modeling, and collaboration with a diversity of experts to inform decisions regarding the most important lands to conserve. To this end, Ag + Open Space led and managed the Sonoma County Vegetation Mapping and Lidar Program (Sonoma Veg Map Program) to create a suite of datasets to inform its land conservation objectives, supported by a highly qualified team of consultants including the authors of this paper. In addition to Ag + Open Space funding and staff and consultant contributions, substantial funding and guidance was provided by a consortium of organizations including NASA, California Department of Fish and Wildlife, California Native Plant Society, United States Geological Survey and the Sonoma County Water Agency, as well as two technical committees. In May of 2017, Ag + Open Space completed and provided public access to a robust and comprehensive suite of fine-scale landscape datasets for the entirety of Sonoma and portions of Mendocino Counties.

Based on 2013 high resolution imagery, lidar data and field samples, the datasets provide fine-scale information about the County's topography, land use, vegetation, and hydrology. Specific datasets important for landscape planning and land conservation include forest metrics, digital surface and digital elevation models, ortho-photography, watershed boundaries, flow accumulation/direction, lifeform, croplands, fine-scale vegetation maps, pervious/impervious surfaces, high resolution building footprints, contours, stream centerlines, and aboveground biomass and carbon. These data are available for download at the Ag + Open Space site sonomavegmap.org.

Sonoma Complex Fires

Wildfires are an integral part of life in Sonoma County and multiple fires have burned across the Sonoma County landscape over the last century (Figure 2). However, over the last decade, the size, frequency, intensity, and costs of wildfires throughout the west have increased as a result of a century of fire exclusion, global climate change, and increased construction in the wildland urban interface (Mitchell 2013; Syphard and Keeley 2015; Mann et al. 2016). On the evening of 8 October 2017, the Tubbs, Nuns, and Pocket Fires (termed the Sonoma Complex Fires) ignited and burned for 20 days, leaving 44,800 ha (110,700 acres) burned, 6,997 structures destroyed, and causing 24 fatalities in Sonoma and Napa Counties.

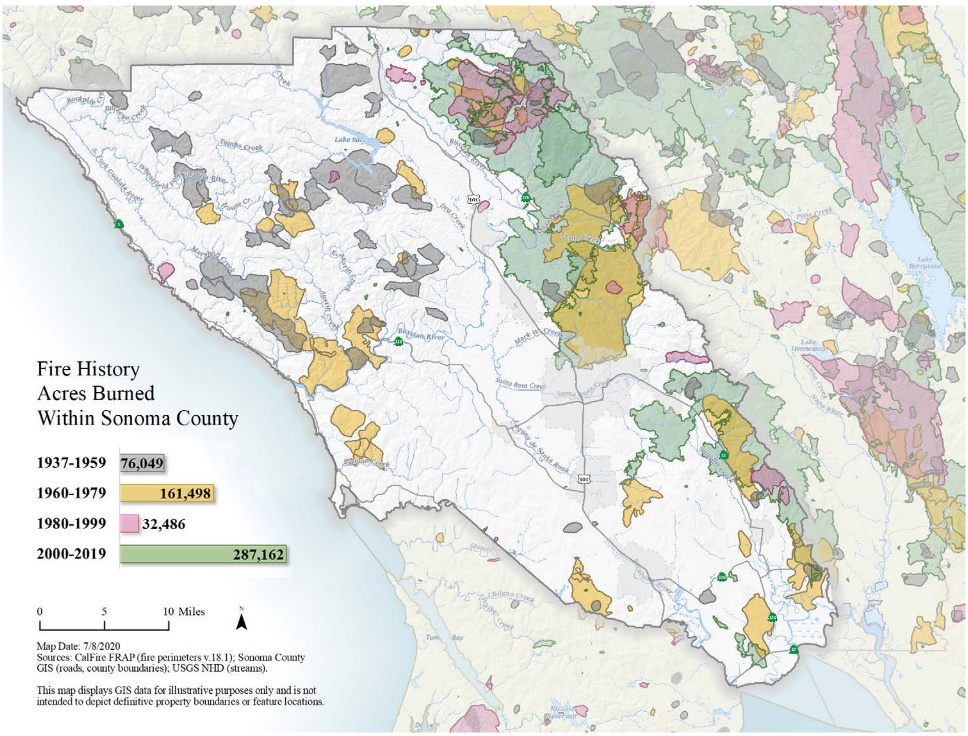

Figure 2. Fire perimeters in Sonoma County and vicinity between 1937 and 2019. Source: Fire and Resource Assessment Program (FRAP) fire perimeter layer developed by BLM, CAL FIRE, NPS, and USFS.

Research objectives

To better plan for future wildfire events and mitigate wildfire risk, Ag + Open Space sought and received NASA Rapid Response Research funding (grant number 80NSSC18K0683) to employ the Sonoma Veg Map Program and other datasets to better understand the Sonoma Complex Fires. Research tasks included: (1) mapping woody canopy condition (percent woody canopy damage) as a result of the 2017 fires from pre- and post-fire imagery and lidar data; and (2) discovering and quantifying relationships between post-fire woody canopy condition and landscape characteristics such as weather, vegetation type, fuel loading, land use, and land management patterns. The results of these analyses are being used to inform strategies for land conservation, land use, and land management activities that enhance ecosystem and human community resiliency to wildfire.

This paper summarizes the methods and results of the research effort, and presents the major project conclusions. The first section reviews the methods used to accomplish each research task. The second section reports on research results, and the final sections discuss the impact of the results and present thoughts for future research.

METHODS

Study area

The study area includes portions of the Nuns, Tubbs, and Pocket fires that burned within Sonoma County in 2017 plus portions of Napa County captured by the imagery (Figure 3). All three fires are located primarily in the eastern mountains of Sonoma County. The Pocket fire was located within the Big Sulphur Creek and Middle Russian River watersheds in the northern Mayacamas Mountains, draining into the Alexander Valley. The Tubbs fire was located within the Middle Russian River and Mark West Creek watersheds, with portions of the fire extending into urban areas within the city of Santa Rosa. The Nuns fire was situated in the Sonoma Creek, Napa River, and Carneros Creek watersheds on the west and east flanks of the southern Mayacamas Mountains and portions of the Sonoma Mountains. Areas that burned east of Santa Rosa are within the Santa Rosa Creek watershed. Terrain of the study areas ranges from flat to steep with elevations ranging from 60 to 1,050 m. Vegetation across the study areas is largely comprised of oak woodland, mixed chaparral, mixed hardwood/conifer forest, grassland, and vineyards.

Post-fire woody canopy condition mapping

The first step of this project was to map woody canopy condition following the Sonoma Complex Fires. We acquired 0.305 m (1 foot) resolution stereo, digital airborne, 4-band (red, green, blue, near-infrared) optical imagery over the areas of the Pocket, Tubbs, and Nuns fires in Sonoma County (Figure 4). The imagery was collected using a Vexcel UltraCam Eagle M3 camera flown at 5,054-m (1-foot) altitude on a Beechcraft Airliner twin turboprop aircraft. Airborne imagery was selected over satellite imagery because it can be collected cloud-free and carries no license restrictions, allowing the imagery to be freely shared in the public domain. The imagery was flown by Quantum Spatial (quantumspatial.com) in June of 2018, and provides a smoke- and cloud-free view of all areas within the footprint of the Sonoma Complex Fires in Sonoma County. Following quality control, the post-fire imagery was made available to the public on sonomavegmap.org.

We evaluated the condition of woody canopy for vegetation communities mapped in the Sonoma County Fine-Scale Vegetation and Habitat Map, which characterizes 82 classes of land use and vegetation across the county at the alliance-level with minimum mapping

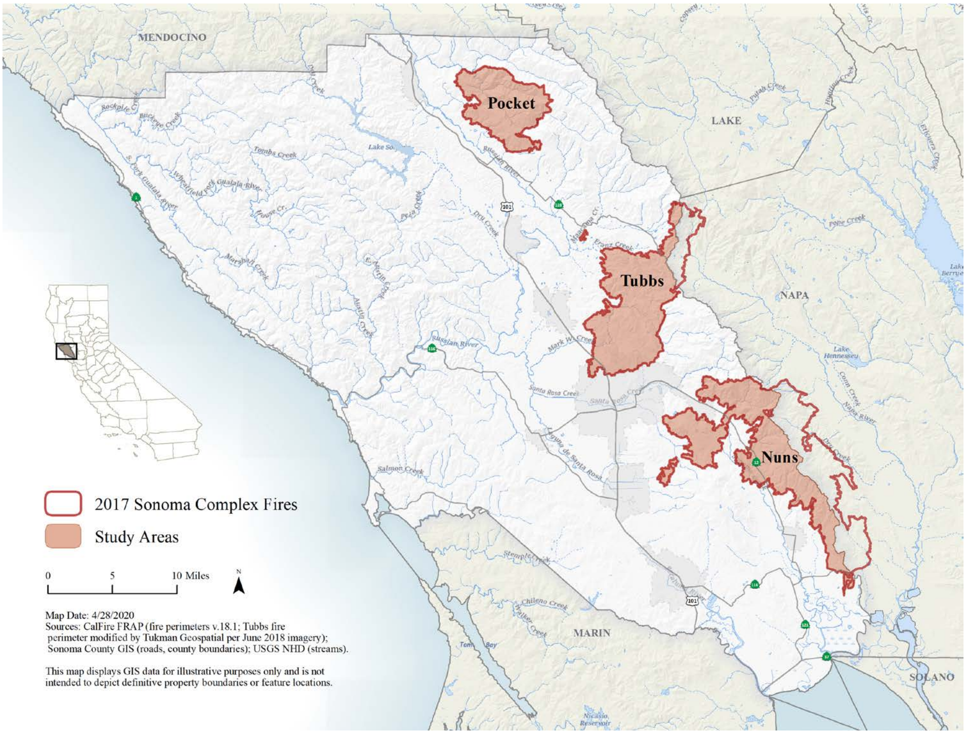

Figure 3. The study areas include portions of the Sonoma Complex Fires within Sonoma County, CA.

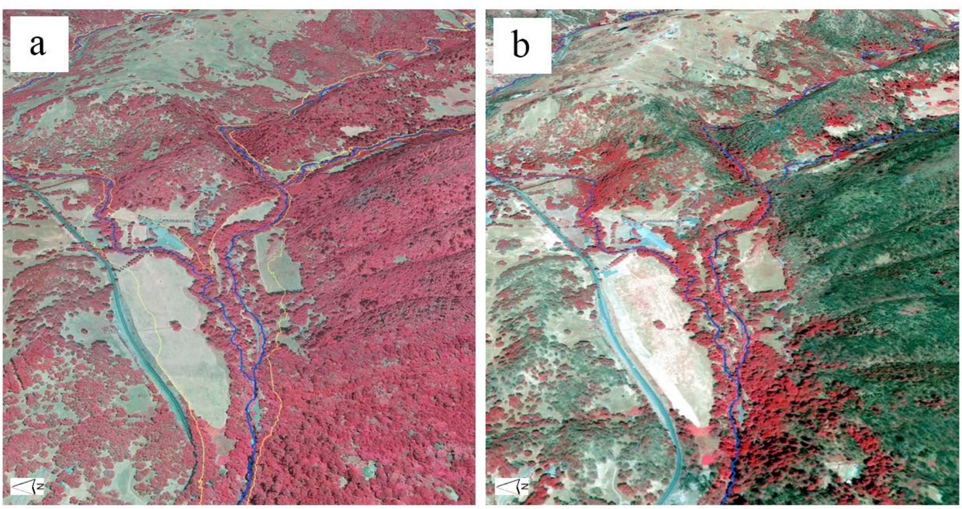

Figure 4. Comparison of 2013 pre-fire imagery (a) to the 2018 post-fire infra-red imagery (b) for the Mark West Creek area of Sonoma County.

units ranging from 0.1–0.4 ha (0.25–1 acre). Please see the Sonoma Vegetation and Habitat Map Final Report for descriptions of each of the map classes (https://sonomaopenspace.egnyte.com/dl/1SWyCSirE9/).

First, due to variability of post-fire woody canopy condition within the fire-affected polygons of the Sonoma County Fine-scale Vegetation and Habitat Map, we created ¼ to 20 acre homogenous sub-polygons based on similar Normalized Difference Vegetation Index (NDVI) values in post-fire imagery using Trimble's eCognition software (http://www.ecognition.com/suite) (Figure 5d).

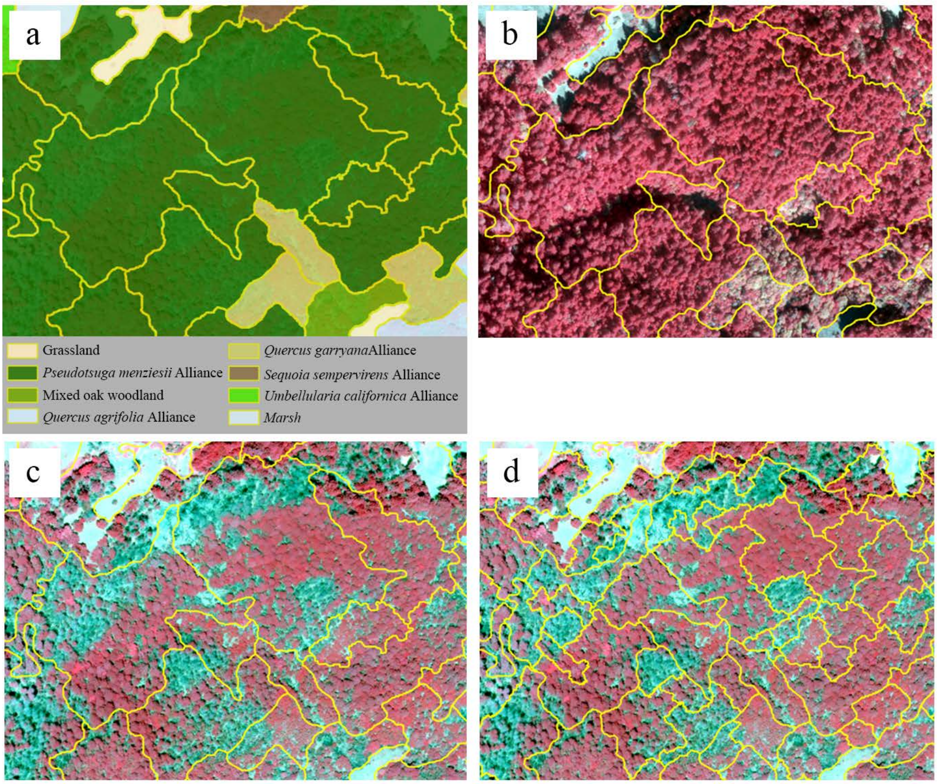

Figure 5. Comparison of the fine-scale vegetation map polygon classes (a), to the fine-scale vegetation polygons over pre-fire 2013 infrared imagery (b), over post-fire 2018 imagery (c), and the sub-polygons of homogeneous damage within the fine-scale polygons (d).

Next, we quantified percent damage of each sub-polygon by calculating the relative proportion of burned versus unburned canopy based on NDVI values from the post-fire imagery. To do this, we further broke the sub-polygons into tiny segments (approximately 0.5-5.5 m^2) in eCognition based on NDVI value (Figure 6a), and classified them as shadowed or illuminated using the average near-infrared band value of the tiny segments. Segments with low near-infrared values were classified as shadowed and segments with high near-infrared were classified as illuminated.

Finally, we established NDVI and Visual Atmospheric Resistance Index (VARI) thresholds to classify the segments as burned versus unburned. Because the thresholds differed for shadowed verses illuminated segments, the thresholds were identified through the use of density slices. Density slicing is the process of binning the range of one band or derivative band of imagery into different classes depending on both the distribution of band values and visual interpretation of the imagery. We then applied separate NDVI/VARI density slices on the illuminated and shadowed tiny segments to label each segment as having damaged or undamaged post-fire woody canopies (Figure 6b). In the NDVI histogram of the Pocket Fire there is a clear bimodal distribution of values distinguishing burned from unburned woody canopies (Figure 7). The histograms of the Tubbs and Nuns Fires are similarly bimodal. We calculated percent woody canopy damage for each sub-polygon based on the relative area of burned tiny segments to unburned tiny segments within a sub-polygon.

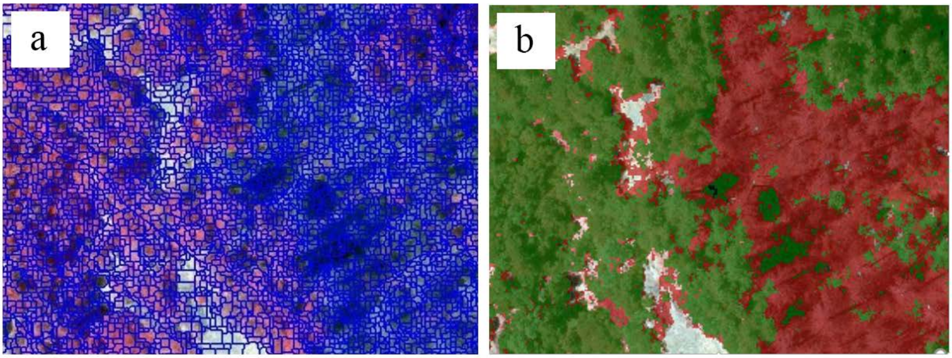

Figure 6. Tiny segments within the sub-polygons (a), and the resulting classification of the tiny segments into burned (red) and unburned (green) vegetation (b).

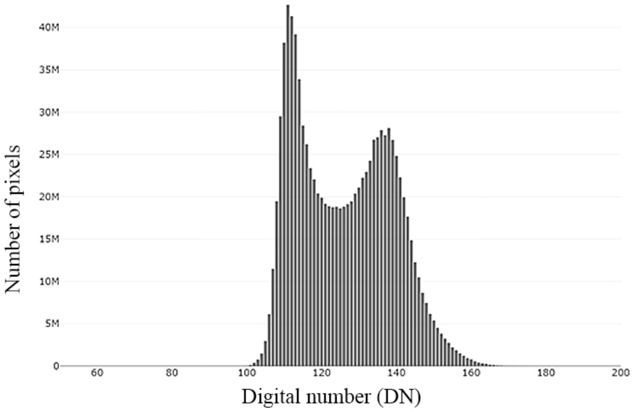

Figure 7. Histogram of NDVI values (converted to a scale from 0-255 and represented as a digital number) for the post-fire imagery of the Pocket Fire area showing a clear bimodal distribution. Damaged canopies have lower NDVI values than undamaged canopies.

Due to the acquisition of aerial imagery in spring following the fire—a time when grasses and forbs have already sprouted and are thus captured as unburned in the post-fire imagery—this project focused on assessing only woody canopy condition within the study area. As a final step in developing the canopy damage maps, we used the 2013 lidar digital surface model to segregate pre-fire woody vegetation (i.e., forests and shrublands) from herbaceous areas based on canopy height of each tiny segment. We classified tiny segments with pre-fire vegetation taller than seven feet as woody vegetation and included these tiny segments in the canopy damage maps. We excluded tiny segments with vegetation height lower than seven feet from the canopy damage maps and subsequent analysis.

We performed an accuracy assessment of the woody canopy condition maps by comparing manually interpreted woody canopy condition (measured in 1% cover increments) from the 2013 and 2018 airborne imagery to the canopy condition map labels for 240 sample sub-polygons (Congalton and Green 2019). Forty samples from each of six canopy condition classes (<5%, 5–20%, 20–40%, 40–60%, 60–80%, 80–100%) were randomly selected. To assure that the analysis was not impacted by spatial autocorrelation, samples were not allowed to be within 365 m (1,200 ft) of one another. Overall accuracy of post-fire woody canopy condition classification was 85%.

Analyzing factors influencing fire behavior and outcomes

The first step in this task involved identifying factors known to affect wildland fire behavior so that measures of these factors could be developed from the Sonoma Veg Map Program and other datasets. Early researchers of fire behavior identified that fire behavior is influenced by factors spanning multiple spatial and temporal scales, and that the most indicative factors were measures of vegetation structure, vegetation type, topography, and climate and weather (Fons 1946; Von Wagner 1969; Rothermel 1972, 1983; Andrews 1986).

Fine scale.—At the finest spatial scale, combustion is controlled by available oxygen, heat, and fuels over seconds (McGranahan and Wonkka 2018). Broadening the scale to a forest stand or vegetation patch, fire behavior is determined by the three-dimensional arrangement of vegetation fuels on the ground and in the canopy, topography, and weather over time. Surface fuels are characterized by size classes, and with all else being equal, smaller-sized fuels (e.g., grasses, shrubs, twigs, leaves) burn more quickly than larger downed wood (Rothermel 1972). For example, "flashy" fuels such as dried grass will burn quickly, but with relatively low intensity. Surface fires will spread more readily with drier fuels and higher wind (Agee et al. 2002). In forests, more severe fires occur when flames reach the tree crown. This generally occurs when surface fires create enough energy to preheat and then combust live fuels in the canopy. Crown fires are initiated with "torching" of lower canopy fuels (e.g., branches, leaves, lichen) that "ladder" the fire to the crown. The higher the canopy fuels are above the surface, as determined by crown base height (CBH), or higher canopy moisture content, the less chance of torching (Agee et al. 2002; Agee and Skinner 2005). Once in the crown, the sustained spread of fire to other crowns occurs with high fuel density (i.e., canopy bulk density) and high rate of spread, which increases with wind speed (Agee et al. 2002; Hall and Burke 2006).

Landscape scale.—At the landscape scale of a wildfire, fire behavior is controlled by variation in topography, weather, and the spatial and vertical pattern of fuels (McGranahan and Wonkka 2018). Forested landscapes with heterogenous patches of different fuel types, moisture content, and natural (e.g., riparian areas) or managed surface fuel breaks can slow fire spread (Weatherspoon and Skinner 1996; Agee et al. 2000; Schmidt et al. 2008).

Regional scale.—At the regional scale, constraints on fire behavior and severity are related to mean climate, patterns of ignition, and broad patterns of vegetation that define fire regimes over decades or longer (McGranahan and Wonkka 2018). In their analysis of Western U.S. forested ecoregions spanning years 2002–2015 and including 2,061 unique fires, Parks and colleagues (2018) found that fire severity at these spatiotemporal scales was primarily determined by variables related to live fuels, followed by variables related to fire weather, climate (i.e., 30-year normals), and topography.

Weather is another critical factor that controls the behavior and severity of a wildland fire over a landscape. In the Western U.S., years with high precipitation in winter and spring can promote vegetation growth, thereby increasing fine-fuel loads, while a dry and hot summer and fall can remove moisture from fuels, making them more combustible (Balch et al. 2018). In California, extreme wind events in the fall can exacerbate pre-existing dry conditions that can lead to more severe fires. For example, the most severe damage inflicted by the Sonoma Complex Fires occurred in the first 14 hours, when strong Diablo winds were channeled by topography through a wind corridor, moving through fuels that had built-up during a wet winter—preconditioned for fire by the warmest summer and autumn on record (Nauslar et al. 2018).

Machine learning

Variable development.—Based on information from the literature and from local wildland fire experts, we used machine learning techniques (Kane et al. 2015) to determine the importance of specific spatial variables for predicting percent woody canopy damage. Machine learning is an artificial intelligence method that analyzes sample data to identify patterns in large, diverse datasets. In this project, the dependent variable in each fire analysis was the percent woody canopy damage of each sub-polygon. We created 66 landscape and weather/climate spatial datasets used as independent variables in the machine learning analysis (Table 1).

There are a total of 46,835 woody canopy condition sub-polygons across the study areas. We calculated landscape and weather/climate variables for each of the sub-polygons using python, pandas and arcpy, and stored these data in a table with each row representing a sub-polygon and each column representing the values of one of the 66 independent variables. Many of the variables were derived from topographic and elevation data from the Sonoma Veg Map Program. For example, based on work by Kramer (Kramer et al. 2014, 2016) and Hoff (Hoff et al. 2019) we used LasTools to create a 20-m resolution ladder fuel proxy derived from the Sonoma County 2013 countywide QL1 (8 points per square meter) lidar point cloud. These data provide information about the density of living and dead vegetation in vertical strata between one and four meters, and from four and eight meters above the ground.

The values of cells in the table represented the mean value for the independent variable for that sub-polygon if the independent variable was continuous, and the plurality value if the independent variable was thematic. In addition to the variables characterizing the sub-polygons themselves, a number of independent variables were created for the sub-polygon plus its surrounding neighborhood. These variables were created in the same manner as those

Table 1. Independent variables used in the machine learning analysis. LC = measure of land cover type; T = measure of topography; S = measure of nearness to streams; V = measure of vegetation structure; C = measure of climate/weather condition

Description of Independent Variables	Abbreviation	Measurement Type
[1]Fine-scale vegetation class of the sub-polygon	Veg	LC
[1]Majority fine-scale vegetation class within 1000 ft (304.8 m) of sub-polygon	MajVeg-1000	LC
[1]Majority fine-scale vegetation class within 500 ft (152.4 m) of sub-polygon	MajVeg-500	LC
[3]Percent of sub-polygon that is impervious	%Imperv	LC
[3]Percent of sub-polygon that is structure	%Struc	LC
[1]Percent of area surrounding sub-polygon that is forest within 1000 ft (304.8 m)	%Surr-For-1000	LC
[1]Percent of area surrounding sub-polygon that is forest 500 ft (152.4 m)	%Surr-For-500	LC
[1]Percent of area surrounding sub-polygon that is impervious within 1000 ft (304.8 m)	%Surr-Imperv-1000	LC
[3]Percent of area surrounding sub-polygon that is impervious 500 ft(152.4 m)	%Surr-Imperv-500	LC
[1]Percent of area surrounding sub-polygon that is shrub within 1000 ft (304.8 m)	%Surr-Shrb-1000	LC
[1]Percent of area surrounding sub-polygon that is shrub 500 ft (152.4 m)	%Surr-Shrb-500	LC
[1]Percent of area surrounding sub-polygon that is not forest or shrub within 1000 ft (304.8 m)	%Surr-NoFor-Shrb-1000	LC
[1]Percent of area surrounding sub-polygon that is not forest or shrub 500 ft (152.4 m)	%Surr-NoForShrb-500	LC
[1]Percent of area surrounding sub-polygon that is vineyard within 1000 ft (304.8 m)	%Surr-Vine-1000	LC
[1]Percent of area surrounding sub-polygon that is vineyard 500 ft (152.4 m)	%Surr-Vine-500	LC
[1]Percent of sub-polygon cone area that is vineyard	%Cone-Vine	LC
[3]Percent of sub-polygon cone area that is structure	%Cone-Struc	LC
[3]Percent of sub-polygon cone area that is impervious	%Cone-Imperv	LC
[1]Area of *Eucalyptus* stand nearest to sub-polygon	Area-Euca	LC
[1]Distance of sub-polygon to nearest *Eucalyptus* stand	Dist-Euca	LC
[1]Distance of sub-polygon to nearest conifer stand	Dist-Conif	LC
[1]Distance of sub-polygon to nearest irrigated area	Dist-Irrig	LC
[1]Distance of sub-polygon to nearest knobcone pine stand	Dist-Knob	LC
[1]Distance of sub-polygon to nearest riparian stand	Dist-Rip	LC
[1]Distance of sub-polygon to nearest shrub stand	Dist-Shrb	LC

Table 1 continued

Description of Independent Variables	Abbreviation	Measurement Type
[1]Distance of sub-polygon to nearest structure	Dist-Struc	LC
[2]Percent of sub-polygon burned in fires from 1939–present	%Burn-39-2020	LC
[2]Percent of sub-polygon burned in fires from 1939–1969	%Burn-39-69	LC
[2]Percent of sub-polygon burned in fires from 1970–1991	%Burn-70-91	LC
[2]Percent of sub-polygon burned in fires from 1992–2017	%Burn-92-17	LC
[4]Distance of sub-polygon to nearest property with a conservation easement	Dist-Ease	LC
[4]Distance of sub-polygon to protected lands (park, preserve etc.)	Dist-Prot	LC
[3]Sub-polygon majority aspect	Maj-Asp	T
[3]Sub-polygon majority 32-class slope aspect index	Maj-SlpAsp	T
[5]Topographic index for majority of the sub-polygon	Maj-TopoInd	T
[3]Sub-polygon mean ground elevation	Mn-Elev	T
[5]Topographic index within 1000 ft (304.8 m) of sub-polygon	TopoInd-1000	T
[5]Topographic index within 500 ft (152.4 m) of sub-polygon	TopoInd-500	T
[3]Sub-polygon mean slope from bare earth DEM	Mn-Slp	T
[3]Sub-polygon mean horizontal distance from nearest stream	Mn-DistStr	S
[3]Sub-polygon mean height above river (relative to nearest large stream)	Mn-HtRiv	S
[3]Sub-polygon [# of lidar returns from 1–4m/# of lidar returns from 0–4 m]	Lad-1-4	V
[3][# of lidar returns from 1–4 m /# of lidar returns from 0–4 m] within 1000 ft (304.8 m) of sub-polygon	Lad-1-4-1000	V
[3][# of lidar returns from 1–4 m /# of lidar returns from 0–4 m] within 500 ft (152.4 m) of sub-polygon	Lad-1-4-500	V
[3]Sub-polygon [# of lidar returns from 4–8 m/# of lidar returns from 0–8 m]	Lad-4-8	V
[3][# of lidar returns from 4–8 m /# of lidar returns from 0–8 m] within 1000 ft (304.8 m) of sub-polygon[3]	Lad-4-8-1000	V
[3][# of lidar returns from 4–8 m /# of lidar returns from 0–8 m] within 500 ft (152.4 m) of sub-polygon	Lad-4-8-500	V
[3]Sub-polygon percent canopy density in the 15–60 ft (4.6–18.3 m) range	%CnpDen-15-60	V

Table 1 continued

Description of Independent Variables	**Abbreviation**	**Measurement Type**
[3]Sub-polygon percent canopy density in the 60–100 ft (18.3–30.5 m) range	%CnpDen-60-100	V
[3]Sub-polygon percent canopy density in the 100–150 ft (30.5–45.7 m) range	%CnpDen-100-150	V
[3]Sub-polygon percent canopy density in the 150–200 ft (45.7–61.0 m) range	%CnpDen-150-200	V
[3]Sub-polygon percent canopy density in the 200–250 ft (61.0–76.2 m) range	%CnpDen-200-250	V
[3]Sub-polygon mean absolute canopy cover	Mn-CnpCov	V
[3]Sub-polygon mean canopy height	Mn-CnpHt	V
[3]Sub-polygon mean canopy slope	Mn-CanSlp	V
[3]Standard deviation of sub-polygon canopy cover	SD-CnpCov	V
[3]Standard deviation of sub-polygon canopy height	SD-CnpHt	V
[3]Presence of woody land cover above 6 ft (1.8 m) in height	%Wood>6ft	V
[8]Sub-polygon mean climatic water deficit (September 2017)	Mn-CWD	C
[8]Sub-polygon mean evapotranspiration (1980-2010)	Mn-Evap	C
[6]Sub-polygon mean summer fog (June to August)	Mn-Fog	C
[8]Sub-polygon mean average annual precipitation (1980-2010)	Mn-Precip	C
[6,7]Humidity at the nearest weather station at the time MODIS/VIRS first detected the fire at the sub-polygon	Humid	C
[6,7]Wind direction at nearest weather station at the time MODIS/VIRS first detected the fire at the sub-polygon	WndDir	C
[6,7]Wind speed at nearest weather station at the time MODIS/VIRS first detected the fire at the sub-polygon	WndSpd	C
[6,7]Wind gust speed at nearest weather station at the time MODIS/VIRS first detected the fire at the sub-polygon	WndGustSpd	C

Sources:
[1]Sonoma Veg Map Program Vegetation Products
[2]CAL FIRE
[3]Sonoma Veg Map Program Lidar Products
[4]California Protected Areas Database/ California Conservation Easement Database
[5]California Landscape Conservation Partnership
[6]NASA MODIS/VIIRS
[7]Weather Stations
[8]Basin Characterization Model (270 m) (Flint et al. 2013)

for the sub-polygons, except that the variable values were calculated for areas within a fixed distance radius (152 or 305 m (500 or 1000 ft)) from the sub-polygon and for areas within cones extending a half mile northeast (340 to 120 degrees) from the sub-polygons. Independent variables are grouped into five variable types based on their foundation as follows:

- Measures of land cover type
- Measures of topography
- Measures of nearness to streams
- Measures of vegetation structure
- Measures of climate/weather condition

Initially the sub-polygons were segregated by fire (Nuns, Tubbs, and Pocket fires) and further by the areas where fire progression was wind-driven or not. To determine wind-driven verses non-wind-driven fire areas, we used NASA Moderate Resolution Imaging Spectroradiometer (MODIS) and Visible and Infrared Scanner (VIRS) imagery to map the perimeters of each fire during (1) the extreme wind-driven fire events which spanned from the time of fire ignition on the late evening of 8 October 2017 continuing to early morning on 9 October 2017 and (2) the non-wind-driven fire events which burned from the morning of 9 October 2017 to 18 October 2017 (Figure 8) (Schroeder et al. 2014). Consequently, the machine learning analysis was initially performed separately on six fire events:

- Nuns fire wind-driven event
- Nuns fire non-wind-driven post wind event
- Tubbs fire wind-driven event
- Tubbs fire non-wind-driven post wind event
- Pocket fire wind-driven event
- Pocket fire non-wind-driven post wind event

In addition, the machine learning analysis was performed on a combination of all fires, segregated only by whether the fire was wind-driven or not.

Random Forests Analysis.—Next, we ran a Random Forests (Breiman and Cutler 2014) machine learning regression analysis against the data set to determine which independent variables are most predictive of percent woody canopy damage (measured in 1% increments) resulting from each fire. Random Forests is a supervised ensemble machine learning technique that uses the values of sample data (i.e., training data) to construct multiple decision trees for modelling the relationships between a dependent variable and the independent variables. The final model output of Random Forests is the most common (i.e., modal) prediction from all of the trees (Green et al. 2017).

To complete the analysis, we first implemented multiple runs of Random Forests with R's randomForest package with different parameters (e.g. number of trees, tree depth), and used the caret package to determine the optimal *mtry* parameter for each fire event (i.e., the number of variables available for splitting at each tree node). We chose parameters that resulted in the highest testing accuracy. Second, we ran each of the six fire events through Random Forests 100 times with different random selections of 80% of the sub-polygons for model training and 20% for model testing. Lastly, we calculated the average (for 100 runs per event) R^2 for the linear relationship between predicted and estimated percent woody canopy damage, the root-mean square error (RMSE) of predictions, and the increase in mean squared error of the Random Forests model for when each independent variable was excluded from the model.

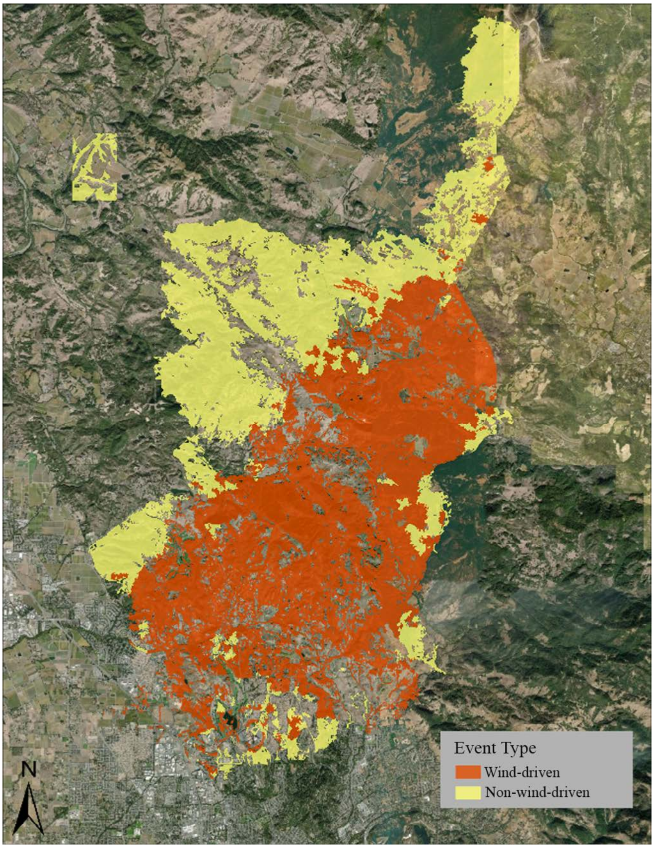

Figure 8. The Tubbs fire segregated into areas that burned during (orange) and after the wind event (yellow).

Finally, we evaluated the importance of each of the 64 independent variables in each of the six fire event models (Genuer et al. 2010). We measured variable importance as the percent increase in mean square error that can be attributed to the exclusion of the variable in the model (Liaw and Wiener 2002). Random Forests calculates this statistic by running the analysis first with the measured value for each variable sample, and then a second time, but letting the value of the variable change randomly. The resulting change in the mean square error measures how the exclusion of a variable decreases the accuracy of the model versus if the variable was included.

RESULTS

Post-fire woody canopy condition mapping

The amount of area in each percent canopy damage classes for the Tubbs and Nuns fires are very similar, with large expanses of higher woody canopy damage; 42–43% of the fire areas are in the 80–100% woody canopy damage percent class. Conversely, the Pocket Fire presents more of a mosaic of woody canopy damage across the landscape with only 19.6 % of the fire area in the 80–100% woody canopy damage percent class (Figure 9).

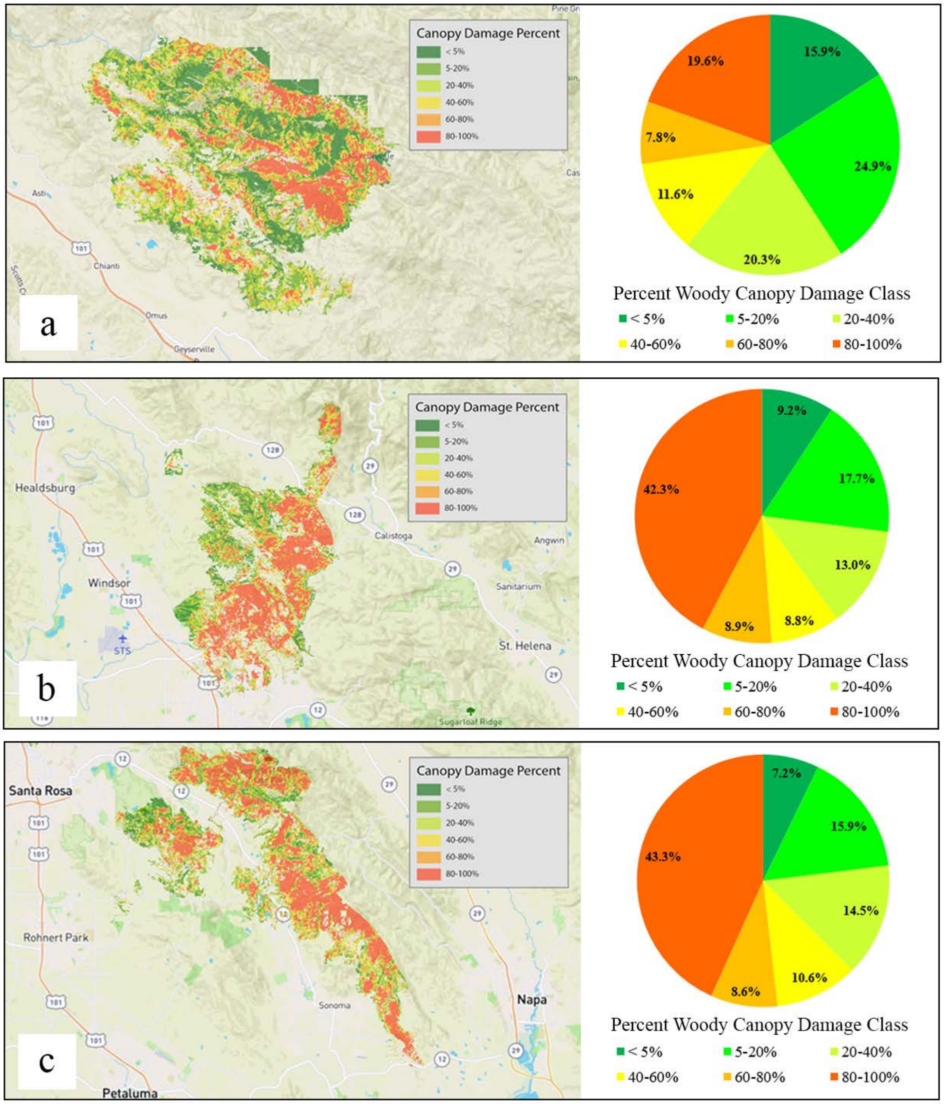

Figure 9. Woody canopy condition maps and proportion of each fire area in each of the percent canopy damage classes for the Pocket (a), Tubbs (b), and Nuns (c) fires. The continuous woody canopy condition values for each of the three fires have been consolidated into percent classes (e.g. <5%, 5–20%, etc.).

Machine learning

Six fire event analysis.— All of the fire events show that a significant amount of variation in woody canopy condition can be explained by the models (Table 2). For each of the six fire events, we determined the 10 most important independent variables in model development and associated percent improvement in mean square error (Figure 10).

Table 2. Comparison of average R^2, RMSE, and MSE for Random Forests models for each of the fire events.

Fire Event	Average R^2	Average RMSE	Average MSE
Nuns Non-Wind	0.55	0.22	0.048
Nuns Wind	0.45	0.24	0.058
Pocket Non-Wind	0.51	0.22	0.048
Pocket Wind	0.50	0.20	0.040
Tubbs Non-Wind	0.56	0.21	0.044
Tubbs Wind	0.52	0.23	0.053

Vegetation structure measures are the most important for all six events and the second most important for all but one event. For example, the ladder fuel metric is 1.5 times more important than the next most important variable (mean canopy height) for the Nuns non-wind-driven event and 1.7 times more important than the next most important variable (horizontal distance to stream) in the Tubbs wind-driven event. Additionally, 32% of the top 10 important variables are measures of vegetation structure.

Climate/weather variables are less important than vegetation structure, but still appear in the top 10 important variables for all six events. Climatic water deficit in 2017, mean evapotranspiration, and wind direction are each listed three times in the top 10 variables. However, wind direction is important only for the non-wind-driven event models which is understandable, as the wind direction during the wind events was fairly constant from the northeast. Measures of how close a sub-polygon is to a stream are in the top 10 important variables for all six events, with the exception of the Tubbs non-wind-driven event. Measures of topography appear as a top 10 variable in only two events. There are more land-cover type variables in Figure 10 than any other variable type, comprising 37% of the ten most important variables. The Pocket wind-driven event is notably different from the other events in that the percent increase in the mean square error attributable to the variables is lower (by a half or a quarter) than that of the top variables of the other events.

While they tend to be less important than vegetation structure measures, there are some additional patterns in the six fire analysis which are of note:

- Distance to nearest *Eucalyptus* polygon is listed as one of the most important variables three times. This was surprising given the small amount of *Eucalyptus* occupying the study area prior to the fires (61 acres).
- Distance to nearest shrub stand appears three times as one of the most important variables.
- Measures of the proximity of a building structure to a sub-polygon appears twice.
- The majority fine-scale vegetation class within 500 or 1000 feet of the sub-polygon appears seven times.
- Distance to knobcone pine stands appears twice.

Combined event analysis.— We removed the stratification of the fires based on location and ran Random Forest on all fires combined, stratifying only by wind-driven or non-wind-driven events. The average variance in the data explained by the models (R^2) increased for both wind- and non-wind-driven events (Table 3), suggesting that the general location of the fires within Sonoma County was not an important factor in fire behavior.

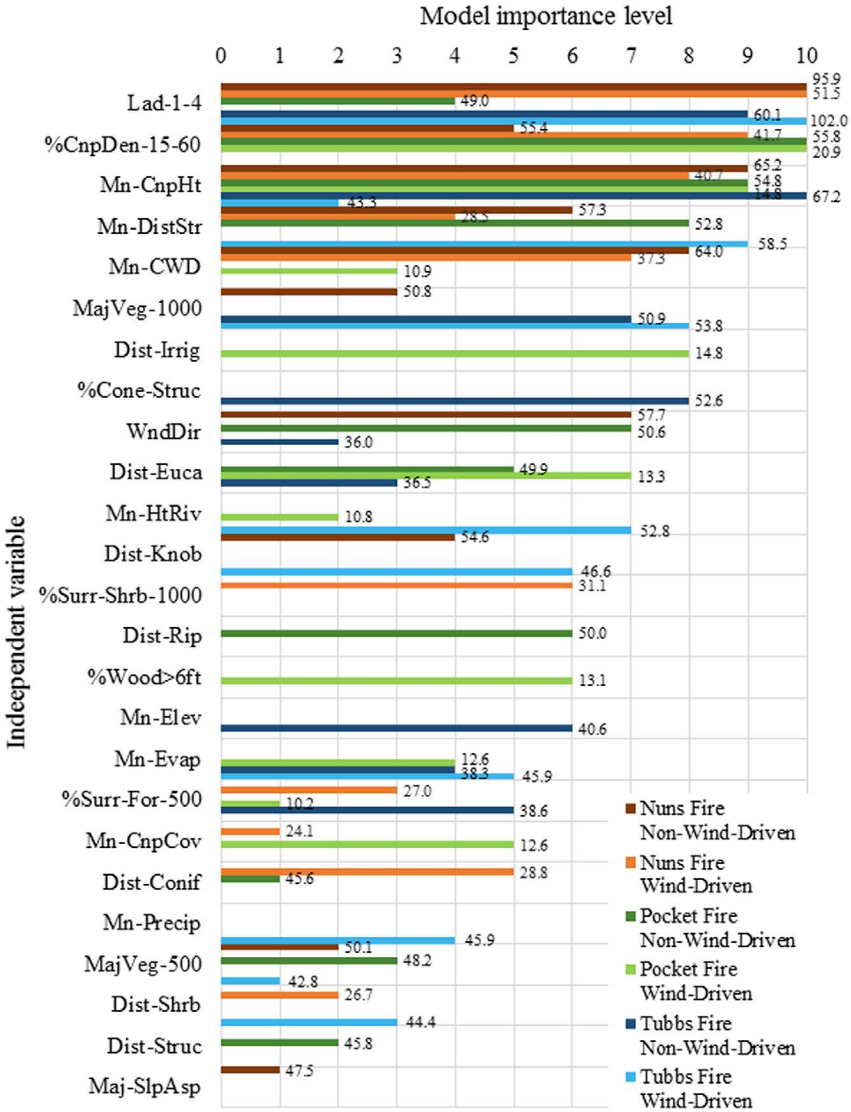

Figure 10. Comparison of the 10 most important independent variables for the six fire events (10 = more important; 1 = less important). Data labels represent the average percent increase in MSE resulting from the exclusion of the variable from the model for 100 runs.

Table 3. Average R^2, RSME, and MSE for the combined fires Random Forests model runs.

Fire Event	Average R^2	Average RMSE	Average MSE
Combined Fires Non-wind-driven	0.63	0.27	0.073
Combined Fires Wind-Driven	0.56	0.29	0.084

For the two-event analysis, where events were stratified by whether or not they were wind- or non-wind-driven, we determined the 10 most important independent variables in model development and associated percent improvement in mean square error (Figure 11). Like the six-event models, measures of vegetation structure, topography, and nearness to streams are the most important variables that affect woody canopy condition, and wind direction is important only in the non-wind event. In contrast to the six-event analysis, the slope-aspect index of the sub-polygon appears at the first (non-wind-driven event) and second position (wind-driven event).

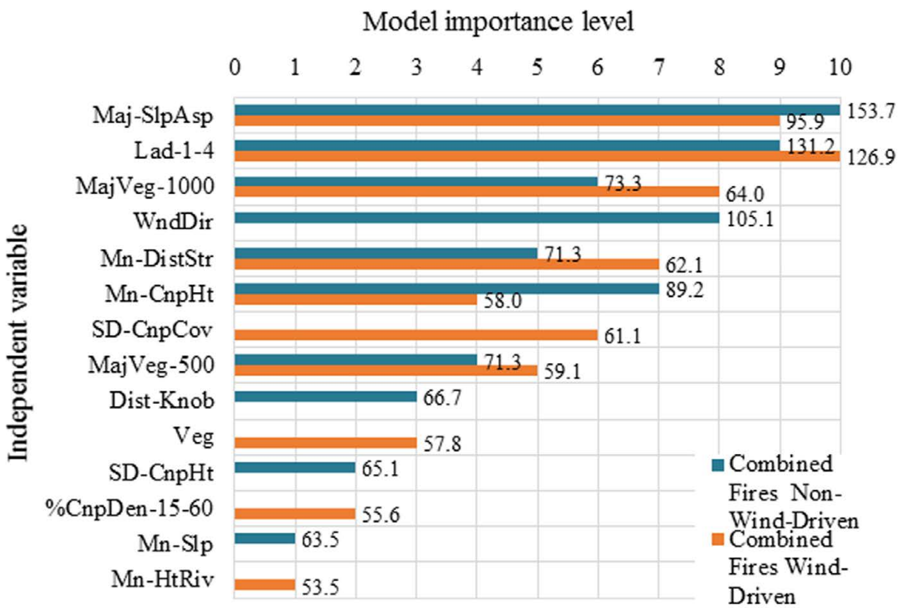

Figure 11. Comparison of the 10 most important independent variables for the two-event analysis (10 = more important; 1 = less important). Data labels represent the average percent increase in MSE resulting from the exclusion of the variable from the model for 100 runs.

There is notably less variability in the measures when comparing the results of the combined fire analysis (Figure 11) versus the six-fire event analysis (Figure 10). For example, only one variable related to nearness to stream appears, rather than the three different variables in Figure 10. Fewer land cover type variables appear to be important and most of those are a measure of the fine-scale vegetation class within 500 or 1000 ft of the sub-polygon. The only climate/weather variable identified as important is wind direction, and it only appears in the non-wind-driven event.

Effect of discontinuous variables

To understand the marginal effect of discontinuous variables, we examined the distribution of the independent variables by percent woody canopy damage. The fine-scale vegetation class is a variant in over 37% of independent variables in Figure 10 (the six event analysis) and in 30% of the variables in Figure 11 (the combined event analysis). Riparian and mesic types have the lowest percent canopy damage, followed by the open hardwood woodland types such as blue oak (*Quercus douglasii*), black oak (*Quercus kelloggii*), valley oak (*Quercus lobata*), and Oregon white oak (*Quercus garryana*). Shrub and upland conifer types exhibited the most percent canopy damage, including fire-adapted knobcone pine (*Pinus attenuata)* and chamise (*Adenostoma fasciculatum)* vegetation alliances (Table 4).

Table 4. Area weighted average canopy damage by fine-scale vegetation class.

Fine-scale Vegetation Map Class	Percent Canopy Damaged
Populus fremontii Alliance	15%
Vancouverian Riparian Deciduous Forest Group	19%
Southwestern North American Riparian Evergreen and Deciduous	26%
Acer macrophyllum Alliance	28%
Southwestern North American Riparian/Wash Scrub Group	30%
Quercus chrysolepis Alliance	30%
Quercus lobata Alliance	31%
Quercus garryana Alliance	35%
Quercus douglasii Alliance	37%
Quercus kelloggii Alliance	38%
Rubus armeniacus Alliance	39%
Arctostaphylos viscida Alliance	41%
Quercus wislizeni (tree) Alliance	43%
Quercus (agrifolia, douglasii, garryana, kelloggii, lobata, wislizenii) Alliance	43%
Non-native Forest & Woodland	48%
Pseudotsuga menziesii Alliance	48%
Aesculus californica Alliance	48%
Quercus agrifolia Alliance	50%
Umbellularia californica Alliance	52%
Arbutus menziesii Alliance	55%
Hesperocyparis sargentii Alliance	55%
Pseudotsuga menziesii - Notholithocarpus densiflorus Alliance	56%
Sequoia sempervirens Alliance	58%
Hesperocyparis macnabiana Alliance	67%
Non-native Shrub	67%
Eriodictyon californicum - Lupinus albifrons Alliance	69%
Pinus sabiniana / Quercus durata Provisional Alliance	70%
Quercus wislizeni (shrub) Alliance	71%
Notholithocarpus densiflorus Alliance	71%

Table 4. continued

Fine-scale Vegetation Map Class	Percent Canopy Damaged
Pinus ponderosa - Pseudotsuga menziesii Alliance	71%
Eucalyptus (globulus, camaldulensis) Semi-natural Alliance	77%
Ceanothus cuneatus Alliance	80%
Baccharis pilularis Alliance	82%
Quercus durata Alliance	83%
Adenostoma fasciculatum Alliance	89%
Californian Mesic Chaparral Group	90%
Arctostaphylos (canascens, manzanita, stanfordiana) A. glandulosa Mapping Unit	93%
Pinus attenuata Alliance	95%
Pinus lambertiana Alliance	99%
Pinus radiata Alliance	99%
Ceanothus thyrsiflorus Alliance	99%

High proportions of the shrubs (88%) and eucalyptus (77%) in the study areas were damaged in contrast to low proportions of riparian hardwoods (20%) and deciduous hardwoods (36%) (Figure 12).

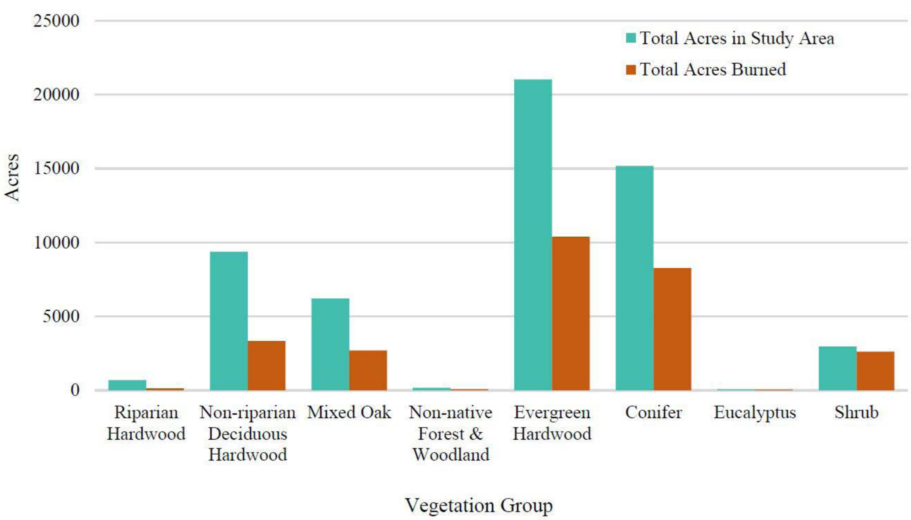

Figure 12. Acres of canopy damage across all fires versus the acres occupied by combined vegetation groups in the study areas before the fires.

While knobcone pine (*Pinus attenuata*) occupies only a small portion of the fire area (1,417 acres or 2.5%), a substantially higher proportion of it (90%) was damaged compared to other conifers such as Douglas fir (*Pseudotsuga menziesii*) (48%) and Sargent cypress (*Hesperocyparis sargentii*) (55%) (Figure 13). Among hardwoods, greater portions of *Eucalyptus* and tanoak (*Notholithocarpus densiflorus*) were damaged, while riparian hardwood communities exhibited the lowest percent woody canopy damage (Figure 14).

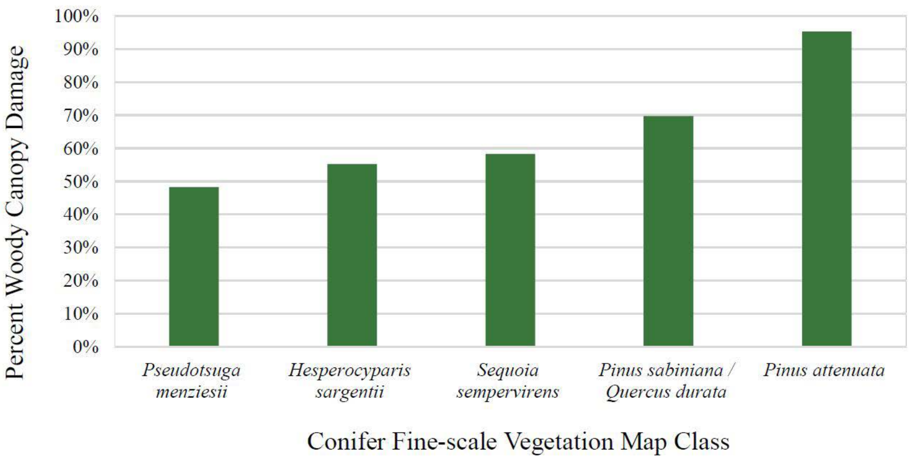

Figure 13. Comparison across conifer vegetation classes of the area damaged by the fires as a percent of total area occupied by the class within the study areas.

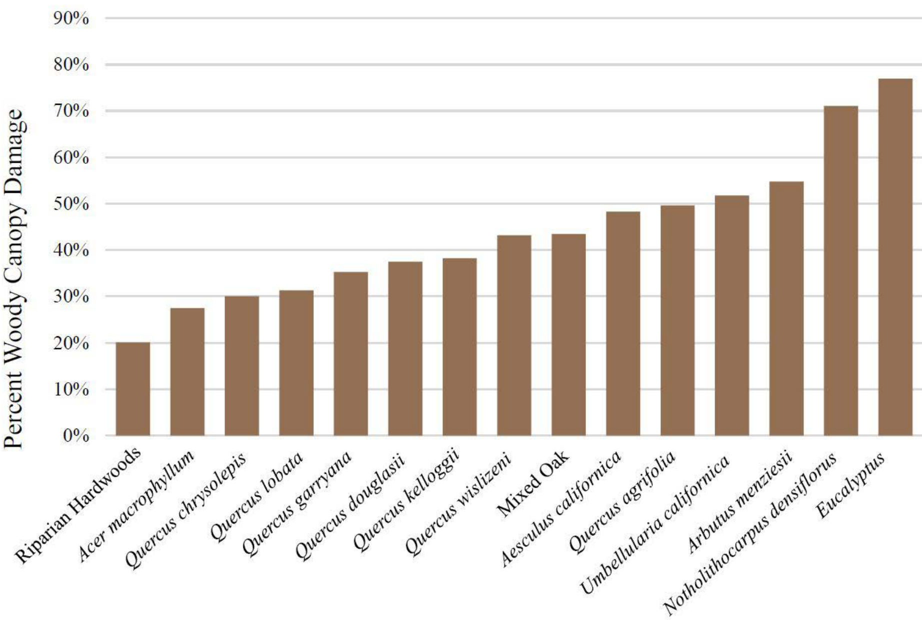

Figure 14. Comparison across hardwood vegetation classes of the area damaged by the fires as a percent of total area occupied within the study areas.

In addition to fine-scale vegetation class, slope-aspect is an important independent variable in the combined event analysis. Sub-polygons with steep south, southwest, and southeast facing slopes experienced the highest percent canopy damage for both the wind-driven and non-wind-driven events (Figures 15 and 16). In addition to ladder fuels, slope

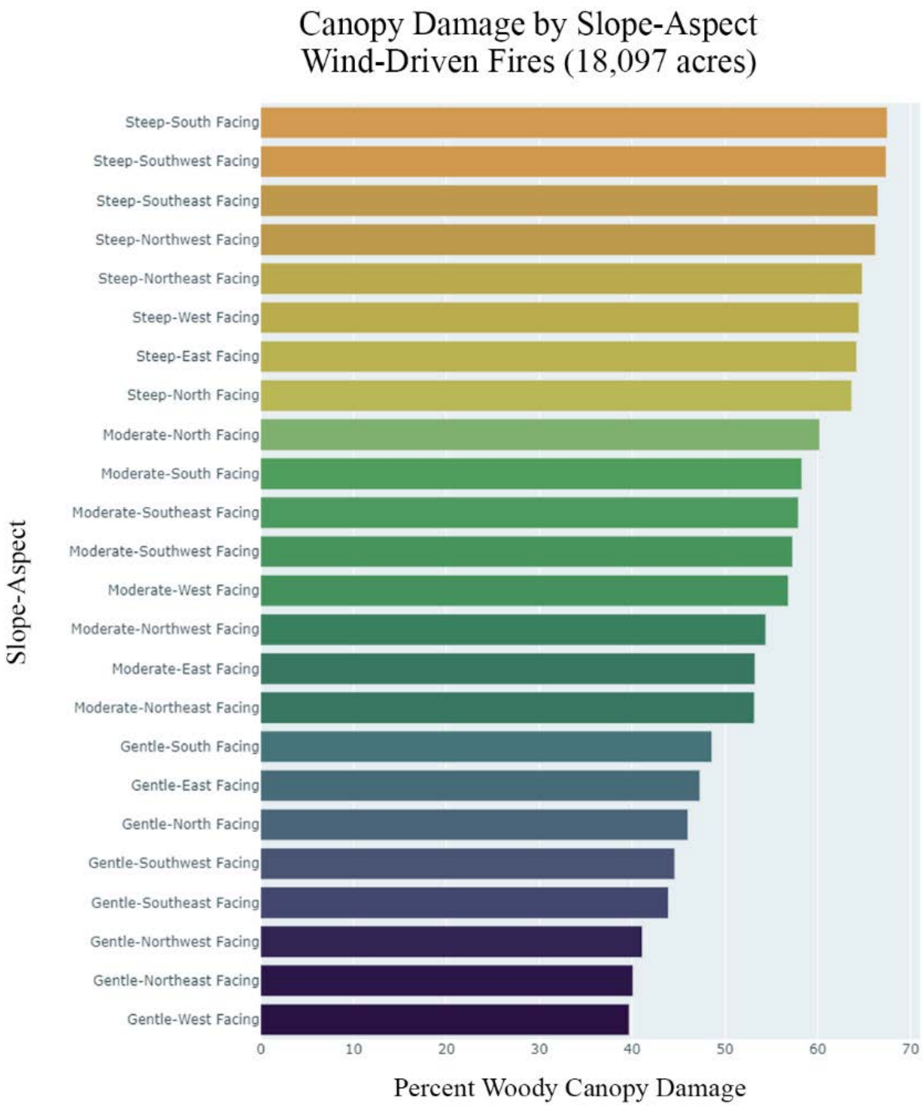

Figure 15. Area weighted average canopy damage by slope-aspect class for the combined wind-driven event.

appears to be the primary driving factor for post-fire canopy condition in the wind-driven fires (Figure 15), with percent canopy damage directly related to slope class—the steeper the slope, the higher the percent damage. Damage in the non-wind-driven fires is much less affected by slope, with steep north and northeast areas sustaining the lowest canopy damage.

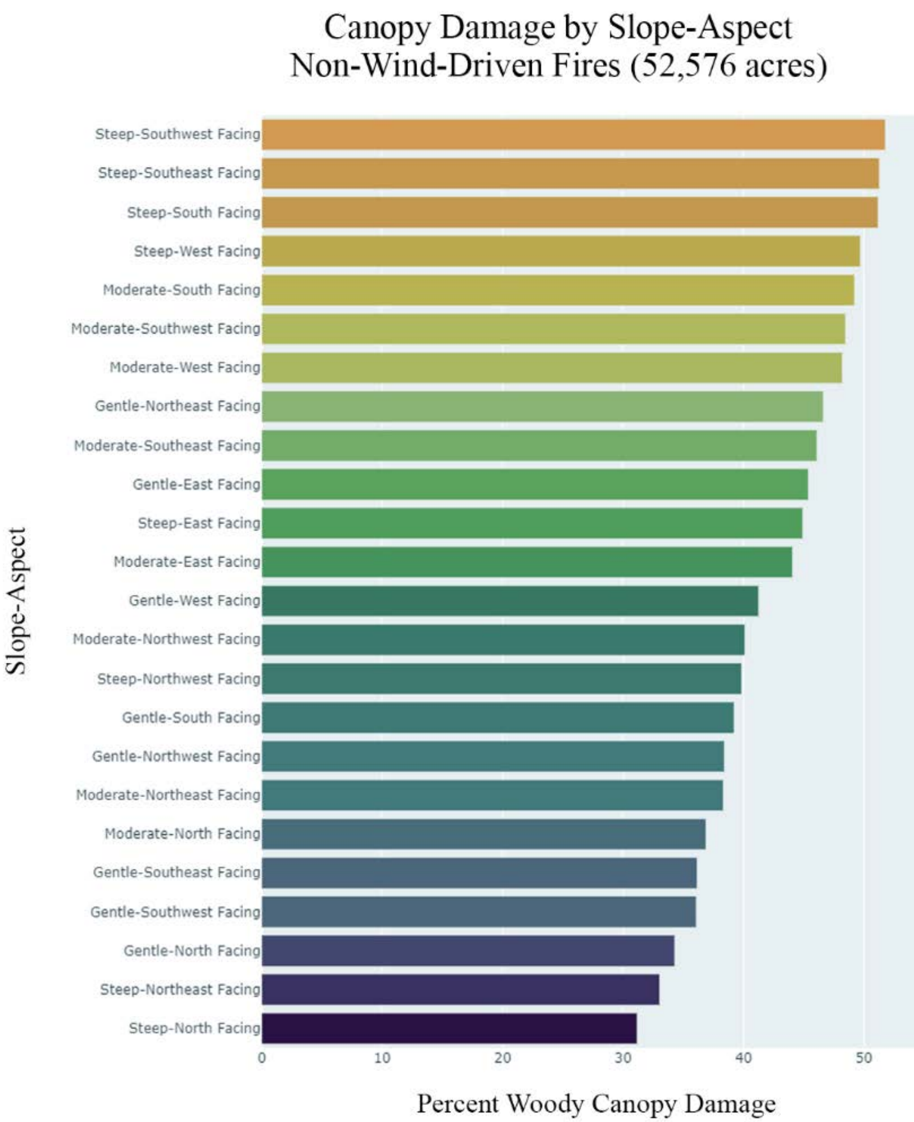

Figure 16. Area weighted average canopy damage by slope-aspect class for the combined non-wind-driven event. Slope was not a strong predictor of damage in non-wind-driven fires.

Effect of continuous variables

To better understand the relationship between the important independent variables and woody canopy condition, we developed partial dependence graphs for the more important continuous independent variables (Figure 17). Partial dependence plots show the marginal effect an independent variable has on the prediction of the dependent variable in Random Forests models, and can help show the direction of the relationship and whether the relationships between dependent and independent variables are linear, quadratic or more complex

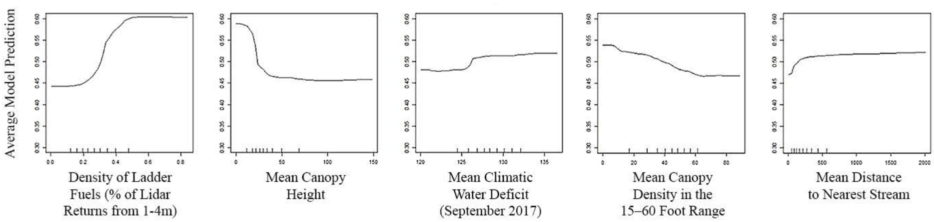

Figure 17. Partial dependence plots for five continuous variables for the six fire events.

(Friedman 2001).

The greater the density of ladder fuels, the higher mean climatic water deficit, and the further away from a stream, the greater the predicted percent canopy damage. The greater the mean canopy height and mean canopy density in the 15–60 ft. range, the lower the predicted percent canopy damage.

Ladder fuels and vegetation type are both important independent variables in all of the machine learning models, and the density of pre-fire ladder fuels varies across vegetation communities within the study area (Figure 18). Knobcone pine (*Pinus attenuata*) and upland shrubs have higher percentages of ladder fuels than other vegetation types in Figure 18, as well as a higher percentage of canopy damage (Table 4).

DISCUSSION

Results of our analysis showed that high resolution airborne imagery and semi-automated techniques can be effectively used to create highly accurate maps of woody canopy condition following a wildfire, and that those maps can be used to better understand how different landscape variables contribute to woody canopy damage from fire. Vegetation structure and type, weather/climate variables, slope, and distance from streams are the primary variables that affect post-fire woody canopy condition in the landscapes of eastern Sonoma County. The higher the density of shrubs and fire-adapted vegetation types, and the higher the density of ladder fuels, the higher the damage. The closer to streams, the lower the damage. During wind-driven fire events, the steepness of slope is also indicative of damage, with steeper slopes experiencing more damage.

Applications for land management, land conservation, land use

The woody canopy condition maps and the replicable approach to mapping and modeling support a wide variety of wildfire recovery and resiliency efforts that protect and

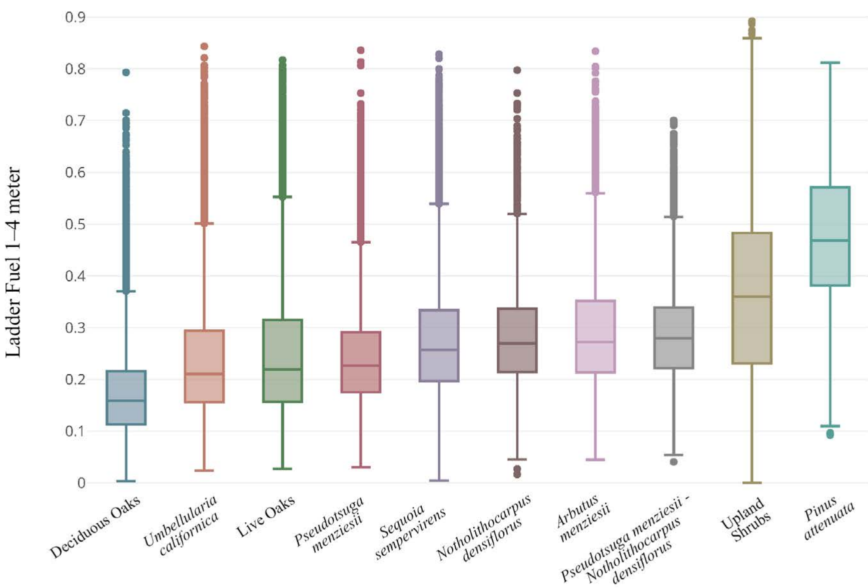

Figure 18. Density of pre-fire ladder fuels by vegetation type within the study areas. Deciduous oaks include blue oak woodland, leather oak chaparral, Oregon white oak woodland, black oak woodland, and valley oak woodland; live oaks include coast live oak woodland, canyon live oak woodland, and interior live oak woodland; upland shrubs include chamise chaparral, hazelnut scrub, Ceanothus chaparral, manzanita chaparral, coyote brush, Californian mesic and maritime chaparral, poison oak scrub, and interior live oak chaparral.

benefit California ecosystems and human communities. Fire behavior experts have long recognized that wildfire behavior is affected by topography, weather, and vegetation type and structure (Finney 1998; Scott and Burgan 2005). This study validates the importance of those variables, but more importantly it offers tools to support the management of those within our control. While we cannot directly manage weather or topography, we can manage wildland fuels, and policy makers can make informed decisions about whether or not valuable assets should be placed in landscapes with heavy fuels and limited access and egress. With this information, we can deploy effective fuel management appropriate for given ecosystem types to promote ecological integrity of the system and support community safety and disaster preparedness. There is neither the funding available nor the need to treat all of the landscape. Now that we can accurately and efficiently map ladder fuels, vegetation type, and vegetation structure, treatments can be prioritized based on the location of heavy fuel loads vis a vis the location of features and assets in need of protection. For example, now that we understand that stream beds are important barriers to fire damage, we can tailor those treatments to account for their importance and the ecological sensitivity of riparian areas. Additionally, fuel reduction efforts such as prescribed or managed fire can be used effectively in these landscapes with less potential damage to nearby structures. Land conservation investments can be targeted in areas of high repetitive fire damage, or in the WUI that surrounds human settlements, and these land conservation easements or fee title purchases can be managed in a way to reduce fuel loading or create fire breaks. Examples of this might include a conservation easement that is intended for cultivated agriculture, grazing, or riparian corridor protection, or a park that has extensive thinning of ladder fuels. Sonoma County Ag + Open Space and other land conservation partners are using the results of this research to prioritize long term conservation investments that support ecosystem and community resiliency and achieve multiple benefits—including sustaining local food supplies, biodiversity, scenic open space, naturally filtered drinking water, as well as positive climate change action related to adaptation, carbon sequestration, and avoided emissions.

Sonoma County, like the State of California, has a strong land use policy focus on infill, combined with a publicly funded land conservation agency that protects working and natural lands. This research provides additional information to inform elected officials and policy makers about how and where development can take place in a way that meets housing demand, protects agricultural and natural lands, supports climate change action and helps to protect public health and safety due to extreme events such as wildfires.

Shared data and shared learning

One of the most important outcomes from this research has been the ability to share data and analysis methods and results with other entities working on related ecosystem and community issues. Starting with the Sonoma Veg Map Program foundational datasets, and continuing on with the research focused on the Sonoma Complex Fires, our data collection and modeling work has been useful beyond the original intent of informing Sonoma County land conservation, land use policy and land management. Lidar and other data from the Sonoma Veg Map Program have contributed to a wide variety of applications including environmental planning, flood risk assessment, carbon mapping, easement monitoring, habitat assessments and ecological restoration, climate adaptation planning, engineering design, agricultural planning, and scientific research (Green 2017).

This research has enhanced the capacity of conservation organizations, land managers, decision makers, and the public to understand the relationships between landscape characteristics, weather, and wildfire-caused woody canopy damage. As a result, public policy, public outreach strategies, and land conservation and management practices are being modified and informed by the findings of this research. The subsequent canopy condition and fire modeling datasets are supporting multiple applications including the prioritization and location of fuels reduction and vegetation management projects, public safety and evacuation route analysis, and land conservation prioritization. Additionally, the findings from this research have helped spur other regions such as the North Coast and Sierra Nevada, as well as other Bay Area counties (including Santa Clara, San Mateo, Marin, and Santa Cruz) and CAL FIRE to build fine-scale landscape datasets, in part, so they can better plan for, manage, and mitigate future extreme wildfire events.

Recommendations for additional research and analysis

Expand statistical analysis.—This project benefitted from an abundance of high-quality spatial data available in Sonoma County. The data created through the Sonoma Veg Map Program provided detailed datasets available in few other places in the country and this research would not have been possible without it. Yet even with the plethora of data available for inclusion in the modeling, the models do not fully explain the observed variance and relationship between woody canopy condition and the landscape and weather variables included in the study. More research and funding are needed to determine additional landscape variables that might improve the models, including measures of surface fuels and land management history (including the use of grazing for fuel management). In addition, our research evaluated the importance of vegetation type in predicting canopy damage, but additional research is needed to better understand the impact of the vegetation type variables. Closeness to vegetation type repeatedly appears as an important variable that influences woody canopy condition, but which of those vegetation types increases or decreases the likelihood of woody canopy damage is not fully understood. The distance to vegetation type variables need to be parsed apart (i.e., into groups such as fire-adapted species, versus riparian species, deciduous oaks, shrubs, etc.) and studied in more depth.

Expand scope of study.—This research focused on the variables that impact damage to the woody canopies of forests and shrublands, but additional research is needed to analyze the landscape variables that contribute to building structure damage. Further, fire modeling is just one application for these datasets—there are other critical issues related to extreme events, ecosystem health and community safety that also rely on these types of data, and additional work is needed to identify landscape datasets that are relevant to multiple climate change and extreme event issues—such as emissions reduction/avoidance, fire, flood, drought, public health and safety—and articulate this need to policy and decision makers.

Expand study across space.— In addition, additional resources are needed to expand the analyses into other ecosystems. This research has provided meaningful analysis for wildfires in eastern Sonoma County, and repeating this research in other ecosystems with different dynamics would be useful in prioritizing fuel treatments in those areas and in determining if any statewide patterns emerge.

This research highlights the importance of lidar data in assessing wildfire risk, and expanding this study beyond Sonoma County is contingent upon lidar data being available. Until recently, many of the variables determined to be important in this study were not measurable, including the ladder fuel metrics, distance from fine-scale streams (i.e., both horizontal and vertical distance from the thalweg of streams at high resolution), mean canopy height, and mean canopy density in the 15 to 60 ft range. Additionally, lidar data are a critical input for the creation of the fine-scale vegetation type map which is also an important independent variable in the canopy condition machine learning analysis. Sonoma County is fortunate that its 2013 QL1 lidar collect was substantially funded by NASA research. The National Oceanic and Atmospheric Administration (NOAA) and the United States Geologic Survey (USGS) have done an admirable job supporting QL2 lidar collects in portions of California, but the USGS cost-sharing requirements are often a high hurdle for rural counties. The broad usefulness and value of lidar data demonstrated by this study points to the need for a partnership between federal and state agencies to complete a statewide lidar dataset.

Expand study across time.— In addition, the damage maps are critical in updating fine-scale vegetation maps for fire damage and providing baseline conditions from which we can further evaluate vegetation impacts over time. More funding is needed to remap the burned areas 3–5 years after the fires to fully understand the mid- and long-term impacts of the fires on the landscape. Finally, this study highlights the need for the development of semi-automated fine-scale change monitoring methods. The methods used in this study were highly successful in mapping woody canopy condition; however, the Sonoma datasets are based on 2013 data which are now seven years old. As other counties in California and regions in the United States migrate to reliance on fine-scale datasets, cost effective methods must be developed for keeping the datasets current. Rather than expensively recreating the datasets from scratch, updating methods should focus only in areas that have changed. Great strides have been made in using Landsat imagery for moderate resolution change monitoring (Huang et al. 2010; Kennedy et al. 2010; Hansen et al. 2013; Zhu and Woodcock 2014). However, fine-scale mapping and monitoring to support local decision making remains expensive, inconsistent, and primarily reliant on manual image interpretation. Research is needed which combines the temporal resolution and scientific calibration of Sentinel and Landsat imagery with the high spatial resolution of commercial imagery to monitor change at fine-scales.

ACKNOWLEDGEMENTS

This project would not have been possible without NASA support in the form of a Rapid Response & Novel Research in Earth Sciences grant (grant 80NSSC18K0683 [K. Gaffney, Principal Investigator]) and technical input and project support from V. Ambrosia, D. Green, W. Turner, and L. Friedl (NASA). We additionally want to thank C. Rice (Wildland Resource Management) for her input on which landscape, vegetation, and weather/climate variables to include in the machine learning analysis and M. Kelly and D. Ackerly (UC Berkeley) for their guidance on the machine learning analysis.

The Sonoma County Vegetation Mapping and Lidar Program, a foundation of this research, was a multi-year effort made possible by the financial, technical, and in-kind support of NASA and the University of Maryland (grant NNX13AP69G from NASA's Carbon Monitoring System [R. Dubayah and G. Hurtt, Principal Investigators]), CDFW and the Vegetation Classification and Mapping Program (VegCAMP), CNPS, USGS, the Sonoma County Water Agency, Sonoma County Information Systems Department, Sonoma County Transportation and Public Works Department, The Nature Conservancy, the City of Petaluma, Save the Redwoods League, and the San Francisco Estuary Institute. We thank members of the Ecology and Botany Group and the Vegetation Mapping and Remote Sensing Advisory Committee for their technical input and expertise.

Author Contributions

Conceived and designed the study: K Green, MT, AS, and K Gaffney
Collected the data: MT and DL
Performed the analysis of the data: MT, DL, and K Green
Authored the manuscript: All authors
Provided critical revision of the manuscript: All authors

LITERATURE CITED

Agee, J. K., B. Bahro, M. A. Finney, P. N. Omi, D. B. Sapsis, C. N. Skinner, J. W. Van Wagtendonk, and C. P. Weatherspoon. 2000. The use of shaded fuelbreaks in landscape fire management. Forest Ecology and Management 127:55–66.

Agee, J. K., C. S. Wright, N. Williamson, and M. H. Huff. 2002. Foliar moisture content of Pacific Northwest vegetation and its relation to wildland fire behavior. Forest Ecology and Management 167:57–66.

Agee, J. K., and C. N. Skinner. 2005. Basic principles of forest fuel reduction treatments. Forest Ecology and Management 211:83–96.

Andrews, P. L. 1986. BEHAVE: Fire Prediction and fuel modeling systems – burn subsystem. Part 1. USDA Forest Service. General Technical Report INT-194.

Balch, J. K., T. Schoennagel, A. P. Williams, J. T. Abatzoglou, M. E. Cattau, N. P. Mietkiewicz, and L.A. St. Denis. 2018. Switching on the Big Burn of 2017. Fire 1:17.

Breiman, L. and A. Cutler, 2014. Available from: https://CRAN.R-project.org/package=randomForest

CAL FIRE. 2019. Top 20 most destructive California wildfires. Available from https://www.fire.ca.gov/media/5511/top20_destruction.pdf (April 2020)

Congalton, R. G., and K. Green. 2019. Assessing the Accuracy of Remotely Sensed Data: Principles and Practices. CRC Press, Boca Raton, FL, USA.

Hall, S. A., and I. C. Burke. 2006. Considerations for characterizing fuels as inputs for fire behavior models. Forest Ecology and Management 227:102–114.

Finney, M. A. 1998. FARSITE: Fire Area Simulator – model development and evaluation. USDA Forest Service, Rocky Mountain Research Station, Research Paper RMRS-RP-4, Revised 2004.

Flint, L. E., A. L. Flint, J. H. Thorne, and R. Boynton. 2013. Fine-scale hydrologic modeling for regional landscape applications: the California Basin Characterization Model development and performance. Ecological Processes 2:25.

Fons, W. T. 1946. Analysis of fire spread in light forest fuels. Journal of Agricultural Research 73:93–121.

Friedman, J. 2001. Greedy function approximation: the gradient boosting machine. Annals of Statistics 1189–1232.

Genuer, R., J. M. Poggi, and C. Tuleau-Malot. 2010. Variable selection using random forests. Pattern Recognition Letters 31:2225–2236.

Green, K., R. J. Congalton, and M. Tukman. 2017. Imagery and GIS. Best Practices for Extracting Information from Imagery. Esri Press, Redlands, CA, USA.

Green, K. 2017. Use and Value of Sonoma County's Vegetation Mapping and Lidar Program Products. Available from: https://sonomaopenspace.egnyte.com/dl/S3thL-9bOsb/ (April 2020)

Hansen, M. C., P. V. Potapov, R. Moore, M. Hancher, S. A. Turubanova, A. Tyukavina, D. Thau, S. V. Stehman, S. J. Goetz, T. R. Loveland, A. Kommareddy, A. Egorov, L. Chini, C. O. Justice, and J. R. G. Townshend. 2013. High-resolution global maps of 21st-century forest cover change. Science 342:850–853.

Hoff, V., E. Rowell, C. Teske, L. Queen, and T. Wallace. 2019. Assessing the relationship between forest structure and fire severity on the North Rim of the Grand Canyon. Fire 2:10.

Huang, C., S. N. Goward, J. G. Masek, N. Thomas, Z. Zhu, and J. E. Vogelmann. 2010. An automated approach for reconstructing recent forest disturbance history using dense Landsat time series stacks. Remote Sensing of Environment 114:183–198.

Kane, V. R., C. A. Cansler, N. A. Povak, J. T. Kane, R. J. McGaughey, J. A. Lutz, and M. P. North. 2015. Mixed severity fire effects within the Rim fire: relative importance of local climate, fire weather, topography, and forest structure. Forest Ecology and Management 358:62–79.

Keane, R. E., K. C. Ryan, T. T. Veblen, C. D. Allen, J. Logan, and B. Hawkes. 2002. Cascading effects of fire exclusion in the Rocky Mountain ecosystems: a literature review. General Technical Report RMRSGTR-91. USDA Forest Service, Fort Collins, CO, USA.

Kennedy, R. E., Z. Yang, and W. B. Cohen. 2010. Detecting trends in forest disturbance and recovery using yearly Landsat time series: 1. LandTrendr – Temporal segmentation algorithms. Remote Sensing of Environment 114:2897–2910.

Kramer, H., B. Collins, M. Kelly, and S. Stephens. 2014. Quantifying ladder fuels: a new approach using Lidar. Forests 5:1432–1453.

Kramer, H., B. Collins, F. Lake, M. Jakubowski, S. Stephens, and M. Kelly. 2016. Estimating ladder fuels: a new approach combining field photography with Lidar. Remote Sensing 8:766.

Liaw, A., and M. Wiener. 2002. Classification and regression by randomForest. R News 2:18–22.

Mann, M. L., Batllori, E., Moritz, M. A., Waller, E. K., Berck, P., Flint, A. L. and Dolfi, E. 2016. Incorporating anthropogenic influences into fire probability models: effects of human activity and climate change on fire activity in California. PLoS ONE 11(4):e0153589

McGranahan, D. A., and C. L. Wonkka. 2018. Wildland fire science literacy: education, creation, and application. Fire 1:52.

Miller, C. 2012. The hidden consequences of fire suppression. Park Science 28(3):75–80.

Mitchell, J. W. 2013. Power line failures and catastrophic wildfires under extreme weather conditions. Engineering Failure Analysis 35:726–735.

Parks, S. A., L. M. Holsinger, M. H. Panunto, W. M. Jolly, S. Z. Dobrowski, and G. K. Dillon. 2018. High-severity fire: evaluating its key drivers and mapping its probability across western US forests. Environmental Research Letters 13(4):044037.

Nauslar, N. J., J. T. Abatzoglou, and P. T. Marsh. 2018. The 2017 North Bay and Southern California fires: a case study. Fire 1:18.

Rothermel, R. C. 1972. A mathematical model for predicting fire spread in wildland fuels. USDA Forest Service, Intermountain Forest and Range Experiment Station, Research Paper INT-115.

Rothermel. R. C. 1983. How to predict the spread and intensity of forest and range fires. USDA Forest Service. General Technical Report. INT-143.

Schmidt, D. A., A. H. Taylor, and C. N. Skinner. 2008. The influence of fuels treatment and landscape arrangement on simulated fire behavior, Southern Cascade range, California. Forest Ecology and Management 255:3170–3184.

Schroeder, W., P. Oliva, L. Giglio, and I. A. Csiszar. 2014. The New VIIRS 375 m active fire detection data product: Algorithm description and initial assessment. Remote Sensing of Environment 143:85–96.

Scott, J. H., and R. E. Burgan. 2005. Standard fire behavior fuel models: a comprehensive set for use with Rothermel's surface fire spread model. USDA Forest Service, Rocky Mountain Research Station, General Technical Report RMRS-GTR-153.

Smith, A. M. S., C. A. Kolden, T. B. Paveglio, M. A. Cochrane, D. Bowman, M. A. Moritz, A. D. Kliskey, L. Alessa, A. T. Hudak, C. M. Hoffman, J. A. Lutz, L. P. Queen, S. J. Goetz, P. E. Higuera, L. Boschetti, M. Flannigan, K. M. Yedinak, A. C. Watts, E. K. Strand, J. W. van Wagtendonk, J. W. Anderson, B. J. Stocks, and J. T. Abatzoglou. 2016. The science of firescapes: achieving fire-resilient communities. Bioscience 66:130–146.

Syphard, A. D., and J. E. Keeley. 2015. Location, timing and extent of wildfire vary by cause of ignition. International Journal of Wildland Fire 24:37–47.

USDA Forest Service. 2014. Forests of California – Story Map. Pacific Northwest Research Station. Available from: https://usfs.maps.arcgis.com/apps/MapJournal/index.html?appid=5133c9e1d8c246a1807426a9ca6ee264 (April 2020)

Weatherspoon, C. P., and C. N. Skinner. 1996. Landscape-level strategies for forest fuel management. Pages 1471-1492 in Sierra Nevada Ecosystem Project: Final report to Congress. Vol. II. Assessments and Scientific Basis for Management Options. Wildland Resources Center Report No. 37. Centers for Water and Wildland Resources, University of California, Davis, CA, USA.

Zhu, Z., and C. E. Woodcock. 2014. Continuous change detection and classification of land cover using all available Landsat data. Remote Sensing of Environment 144:152–171.

Submitted 30 April 2020
Accepted 22 June 2020
Associate Editor was S. Thomas